Cross-diffractive optical elements for wide angle geometric camera calibration

Simon Thibault,[1,2,*] Aymen Arfaoui,[3] and Pierre Desaulniers[1,2]

[1]*Center for Optics, Photonics and Lasers, Laval University, Québec, QC, G1V 0A6, Canada*

[2]*Department of Physics, Engineering Physics and Optics, Laval University, Québec, QC, G1V 0A6, Canada*

[3]*Department of Geomatics, Laval University, Québec, QC, G1V 0A6, Canada*

**Corresponding author: simon.thibault@phy.ulaval.ca*

Received September 7, 2011; revised November 4, 2011; accepted November 7, 2011; posted November 8, 2011 (Doc. ID 154191); published December 14, 2011

Diffractive optical elements (DOEs) can generate multiple two-dimensional (2D) diffraction grids that can be used to calibrate cameras for photogrammetry. However, several factors limit the accuracy and the functionality of this technique. One of the most important is the DOE fabrication itself. A large DOE with wide 2D fan-out grids is very difficult and costly to develop. Consequently, the calibration is limited to small aperture cameras and/or limited angles. To overcome these problems, we present a low cost solution. We propose to use two large, commercially available, crossed phase DOEs that generate 15 × 15 equally spaced dots. As the DOEs are not perfect, the unwanted secondary diffractive orders are used as calibration targets to expand the calibration field of view. We show that the use of the primary and secondary diffractive orders provides a valuable calibration tool for wide angle aerial cameras. © 2011 Optical Society of America

OCIS Codes: 080.0080, 050.0050, 150.1488.

Camera calibration is a necessary step in many applications, such as visual servoing in robotics [1] and three-dimensional (3D) measurement in photogrammetry [2]. Existing camera calibration techniques can be classified into three methods [3]. The first technique is the traditional calibration where the calibration is performed by using known 3D coordinates targets [4,5]. The second technique, called self-calibration, is performed by using image information only [6]. The third calibration technique is based on active vision. The internal and external parameters are estimated by using images and the controllable camera motion parameters [7].

In the case of digital aerial cameras, the calibration is generally performed by using a large room with hundreds of precisely surveyed targets in it [8]. These targets must be located far enough from the camera to simulate infinity and must be positioned at different distances from the camera to get a 3D effect that would cover the camera's entire field of view (FOV). This setup takes a very large and physically stable room dedicated to that purpose and the targets are never at infinity as in operation, which may produce calibration errors.

To get a compact and accurate calibration setup, it was recently proposed to use a fixed amplitude diffractive optical element (DOE) [9]. The amplitude DOE is used to split an incoming collimated laser beam into a number of two-dimensional (2D) diffractive orders. As the virtual sources, the diffracted points are at infinity, which gives precise calibration targets under a compact package.

Several factors limit the accuracy and the functionality of this technique. One of the most important is the DOE's fabrication. Since the aerial camera has a very wide full FOV (sometimes more than 60 deg for large format sensors), the DOE must generate large fan-out angles. To avoid vignetting (pupil mismatch), the DOE aperture must be large enough to fulfill the entrance pupil of the camera under test. The entrance pupil of the lens is inside the lens housing; consequently, the DOE must be oversized, as shown in Fig. 1. In Bauer *et al.*'s setup [9], the diffractive efficiency must be uniform to generate constant virtual images in order to avoid nonuniformity errors. It is very difficult and costly to get large size 2D DOEs that can generate a uniform grid. Consequently, an amplitude DOE was used with a very high zero order intensity, which limits the application of this technology for calibration purpose.

To overcome these drawbacks, in this Letter, we report for the first time, to the best of our knowledge, the use of twin-crossed one-dimensional (1D) phase DOEs to generate a 2D virtual calibration grid. The 1D DOEs are phase Dammann gratings, which are available on the market with standard but not limited sizes up to 2 in. (5 cm). Moreover, the technology is mature and inexpensive (about $1000 for standard gratings). The number of diffractive orders (dots) should be at least 70, but more than 70 points can be used to improve the results [10]. We show that virtual stars produced by the crossed phase

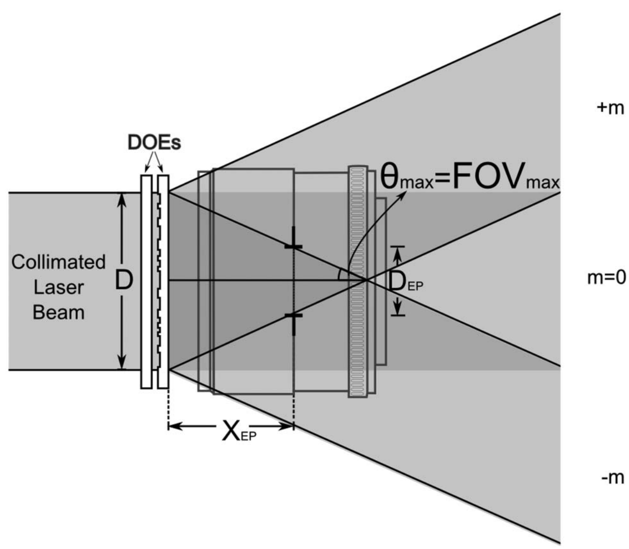

Fig. 1. Overlaps of the DOE orders and entrance pupil position of the camera under calibration.

gratings are efficient to calibrate cameras and provide an aperture large enough to avoid vignetting due to pupil mismatch. We show that the unwanted diffractive orders produced by the gratings are also sufficient to fulfill the entire FOV of the camera and provide enough light to be used as calibration targets. These unwanted diffractive orders are generated by both grating design and fabrication errors. Figure 2 shows a calibration image recorded by the digital camera.

The relation between the required dimensions (D) of the DOE and the entrance pupil position to avoid vignetting depends on the entrance pupil diameter (D_{EP}) of the lens (effective focal length divided by the f-number) and on the lens FOV. This simple relation is defined as follows:

$$X_{\mathrm{EP}} = \frac{D - D_{\mathrm{EP}}}{\tan(\mathrm{FOV})} = \frac{D - \mathrm{EFL}/F}{\tan(\mathrm{FOV})}, \quad (1)$$

where X_{EP} is the distance between the DOE and the entrance pupil. The entrance pupil position is not given by the lens manufacturer but, for most lenses, the entrance pupil is within the lens housing and usually in the middle of the housing. For a wide angle lens with an effective focal length of 45 mm ($f/2.8$) and a 30 deg FOV (full FOV is 60 deg), a 50 mm DOE will require a X_{EP} of 75 mm. Positioning the camera housing within 75 mm of the DOE will be necessary to cover the camera's FOV. For a distance larger than 75 mm, a part of the FOV on the edge will be vignetted. As wide angle lens barrels are smaller than 75 mm, a 50 mm DOE is large enough to calibrate most of the wide angle digital camera.

The use of two crossed gratings also requires a modification of the mathematical representation of the diffracted beams. Equation (3) of Bauer *et al.* [9] is modified to take into account the gratings' clocking errors. As a result of this clocking error, the diffractive orders produced by the first grating are not exactly perpendicular to the orders produced by the second grating. The homogenous coordinates are now obtained as

$$\mathbf{d} = [X, Y, (1 - (X^2 + Y^2)^{1/2}, 0)]^T, \quad (2)$$

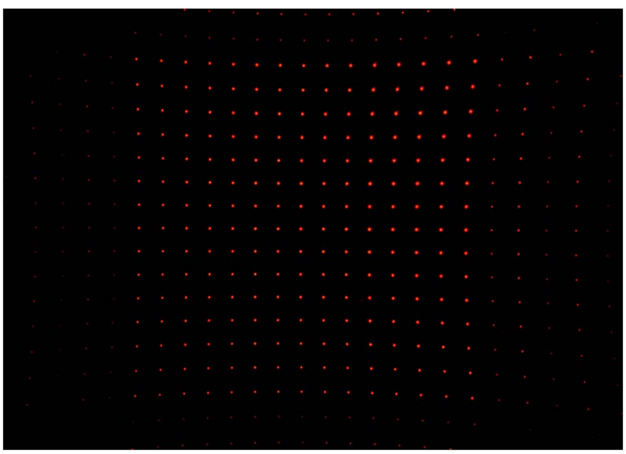

Fig. 2. (Color online) DOE orders calibration grids produced by the cross DOE arrangement (brightness and contrast exaggerated).

$$X = \lambda f_x + r_x + (\lambda f_y + r_y) \cdot \sin(\theta), \quad (3)$$

$$Y = (\lambda f_y + r_y) \cdot \cos(\theta), \quad (4)$$

where f_x and f_y are the grating's spatial frequency, λ is the wavelength of the laser beam, r_x and r_y are the laser beam directions in the x and y directions with respect to the optical axis (z), and θ is the clocking error between the two gratings (in rotation around the z axis).

The calibration setup is illustrated in Fig. 3. A 0.5 mW He–Ne laser (Thorlabs HRR005) is filtered by a spatial filter of 25 μm at the focus of a 20× microscope objective. The laser beam is collimated by a 400 mm achromatic lens (Thorlabs AC508-400-A1). The collimator lens position is adjusted to minimize the collimated beam fringe observed by a shear plate. A neutral density filter (optical density 2.0) is also used to reduce the laser beam's intensity. The collimated beam is then diffracted by the two crossed Dammann gratings (Coherent). The gratings have a 16.4 μm period ($f_x = f_y = 1/16.4\ \mu$m) and a 50.8 mm × 50.8 mm active region. Both gratings generate a dot line of 15 diffractive orders of constant intensity.

To investigate the performance of this new approach, we calibrated a high resolution aerial camera composed of a Phase One $p45+$ digital back and a Mamiya Sekor AF 45 mm $F/2.8$ lens. After aligning the cross gratings to the collimated laser beam, an image of the virtual diffractive object was taken by the camera. The camera integration time and aperture settings were adjusted to record all diffractive orders (primary and the secondary dots). Taking two individual photographs with two different exposure times leads to similar results. We used a centroid algorithm to detect the center with subpixel accuracy of each dot in gray-scale mode, as shown in Fig. 4. The accuracy of the detection of the subpixel position for each diffraction point is an important parameter. We calculated that a centroid error of 1/10th pixel produced a 10^{-5}–10^{-6} relative error on the calibration parameters. From the point intensity distributions, we evaluated a precision of less than 1/20th pixel for this first experiment.

The first calibration was performed using the primary 15×15 central dots. We found a focal length of 45.650 mm. The standard deviation of the residuals between the model and measurement points (15×15) was about 0.13 pixels (0.88 μm). We computed the standard deviation on the entire measurement points (including secondary dots). The residual was about

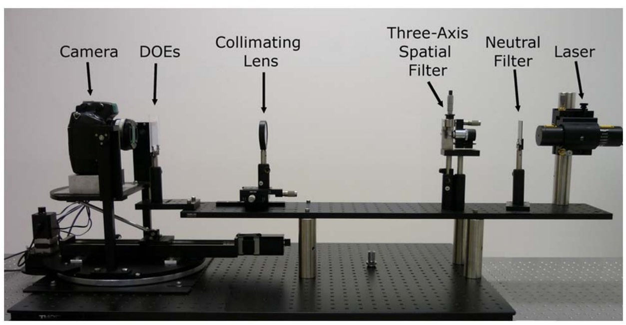

Fig. 3. (Color online) Picture of the calibration setup with the crossed gratings.

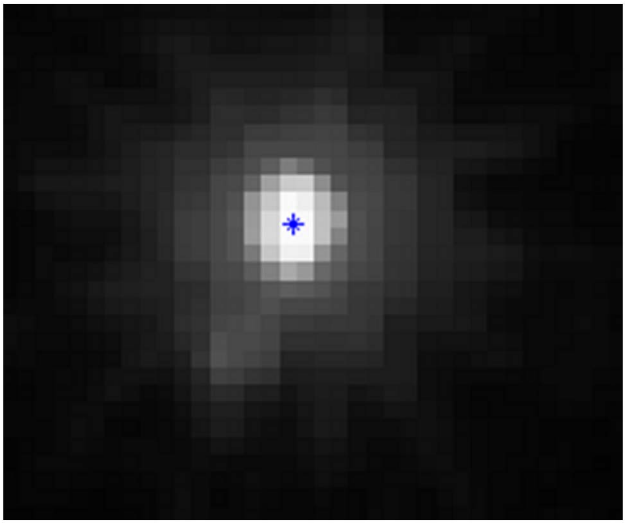

Fig. 4. (Color online) Centroid algorithm results from an arbitrary diffractive order (gray scale).

0.35 pixels (2.38 μm), but with a maximum of more than 3.5 pixels (23.8 μm).

A second calibration was done using the entire diffractive orders both primary and secondary diffraction orders. In that case, we found a focal length of 45.670 mm and the standard deviation of the residuals between the model and measurement points was about 0.22 pixel (1.5 μm). This is a gain of about 40%. Furthermore, the maximum error is reduced to 0.6 pixels (4 μm), which is a gain of more than 6 times. The focal length given in both calibration cases was nearly the same, having less than a 20 μm error. Using secondary orders produced by the crossed gratings helps to determine the standard distortion parameters that clearly required calibration targets on the edge of the image. Distortion varies as the third power of the field; consequently, having at least a few targets on the edge will provide a much higher performance of the calibration process.

In summary, we reported for the first time, to the best of our knowledge, the use of two 1D phase DOEs in a crossed configuration to generate a robust 2D calibration reference tool for geometric calibration of wide angle digital cameras. The new method uses both primary and secondary diffractive orders produced by the crossed Dammann gratings to generate virtual calibration targets. We presented an updated mathematical representation of the diffracted beams with respect to the homogeneous coordinates. The extended calibration grid, using all diffractive orders, provides an efficient calibration tool. We also calculated that, for most wide angle lenses, a 50 mm grating is large enough to prevent vignetting. A simple equation was derived to determine the dimension of the gratings as a function of the FOV and lens barrel dimension for user customization. We identify two limiting factors for the accuracy of the technique. The determination of the diffraction point position requires a smooth intensity distribution to ensure less than 1/10th pixel accuracy. The second parameter is the grating spatial frequency (or period). Further investigation is intended to determine the impact of the accuracy of the grating period on the calibration parameters. We calculated from a first estimation that a period error of ± 0.015 um will produce a 10^{-5} variation on the estimated focal length of the tested objective. The grating period can be measured with nanometer accuracy if required. Finally, this new arrangement is a valuable, low cost, and versatile calibration tool for wide angle aerial camera.

This work is supported by the Natural Sciences and Engineering Research Council of Canada (NSERC) Industrial Chair in Optical Design. The setup was developed under the CIPI-TEN Program supported by XEOS imaging.

References

1. B. Espiau, in Proceedings of ISER, 3rd International Symposium on Experimental Robotics (1993), pp. 187–193.
2. J. Hu, A. Razdan, and J. A. Zehnder J. Atmos. Ocean. Technol. **26** (2009).
3. Q. Wang, L. Fu, and Z. Liu, in Control and Decision Conference (2010), Vol. **35**, pp. 3354–3358.
4. W. Wu and Z. Sun, Appl. Res. Comput. **02**, 04 (2004).
5. J. Heikkila, IEEE Trans. Pattern Anal. Machine Intell. **22**, 1066 (2000).
6. J. Ha and D. Kang, Pattern Recogn. **38**, 143 (2005).
7. Z. Hu and F. Wu, Chin. J. Comput. **25**, 1149 (2002).
8. M. Kroepfl, E. Kruck, and M. Gruber, in *International Archives of Photogrammetry and Remote Sensing* (2004), Vol. **35**, Part B1, pp. 42–44.
9. M. Bauer, D. Grießbach, A. Hermerschmidt, S. Krüger, M. Scheele, and A. Schischmanow, Opt. Express **16**, 20241 (2008).
10. C. Ricolfe-Viala and A. J. Sanchez-Salmeron, Opt. Express **19**, 10769 (2011).